JOC The Journal of Organic Chemistry

Article

pubs.acs.org/joc

An Explicit Interpretation of the Directing Group Effect for the $Pd(OAc)_2$-Catalyzed Aromatic C−H Activations

Lei Zhang and De-Cai Fang*

College of Chemistry, Beijing Normal University, Beijing 100875, China

Supporting Information

ABSTRACT: A comprehensive DFT investigation has been performed for a series of the $Pd(OAc)_2$-catalyzed C−H activations, updating and extending the understanding of directing group effect. In the beginning, the directed and undirected C−H activation mechanisms, based on 10 model reactions, have been discussed comparatively, which disclosed that directing group can exert a thermodynamic driving force, not necessarily a kinetic promotion, on the C−H activation process. Formation of the open palladation species via the undirected pathway is thermodynamically unspontaneous (ΔG = 4−9 kcal/mol), in sharp contrast to that of the cyclopalladation species via the directed pathway (ΔG < 0). Further calculations revealed that the free-energy barriers of proton-transfer are in fact not so high on the undirected pathway (17−24 kcal/mol), while mediation of some O-center groups in the directed pathway would increase the free-energy barriers of proton-transfer. For pyridine *N*-oxide systems, the undirected mechanism was estimated to be more plausible than the 4-member-directed one both thermodynamically and kinetically. In addition, the uncommon 7-membered cyclopalladation has been tentatively explored using two current examples, predicting that electron-rich directing groups can help to stabilize the 7-membered palladacycles formed.

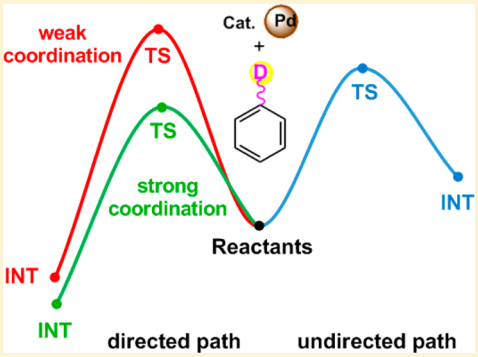

1. INTRODUCTION

C−H bond functionalizations via cyclopalladation in Pd-mediated syntheses provided an alternative, or even a more competitive, strategy to standard organic methods.[1] They displayed a wide prospect of applications to the functionalizations of arenes and heteroarenes, which were very useful in the production of many valuable organic moieties.[2] A general reaction pathway involves in most cases three processes, namely, (a) the regioselective incorporation of the catalyst Pd atom into a substrate C−H bond known as the C−H activation; (b) a group transfer reaction with the coupling partner; (c) usually ending up with the reductive elimination or the β-H elimination to close catalytic cycles and to release coupling-products. The importance of this synthetic methodology has been emphasized in dozens of review papers.[1b,3]

An effective way to achieve the regioselective *ortho*-palladation is based on the complexation assisted C−H activation mediated by directing groups,[1a,4] which refer to a particular class of substrate functionalities bearing appropriate heteroatoms (e.g., O, N, S and P). The complexation between catalysts and directing groups makes an *ortho* C−H bond relatively proximal to metal centers and thus facilitates its activation in a regioselective manner, normally resulting in stable palladacycles. Experimental works confirmed two structural factors of special relevance to reaction efficiencies, including the nature of directing groups and the position of heteroatoms, and the latter unambiguously arose from a strong propensity for formation of the 5-membered or 6-membered palladacycles.[1a] This mechanistic dichotomy toward understanding the directing group effect was one of the main interests in our research group, wherein our previous work[5] focused specifically on the relationships between the type of directing groups and the experimental yield for a series of oxidative Heck reactions.

In most cases, functionalities with an α-heteroatom have not been related essentially with the term of cyclopalladation or directed C−H activation, since the supposed 4-membered palladacycles might have a high degree of strain preventing their formation. A series of experimental works[6] have proved that the aromatics, like anisole, chlorobenzene and their derivatives, were commonly inefficient toward C−H activations by the use of catalytic $Pd(OAc)_2$ or $PdCl_2$. However, they displayed moderate-to-high performance under more demanding reaction conditions, especially using excess aromatic substrates, such as 10 to 100 equiv, or even the cosolvents. Mixtures of *o*-, *m*- and *p*-coupling-products have been isolated,[6] implying that the undirected C−H activation pathway should be plausible with the occurrence of some open palladation intermediates. The nonfunctionalized alkylbenzenes exhibited the similar chemical behavior from the literature reports.[7] Conversely, pyridine *N*-oxides were observed to be compatible, under general synthetic conditions, with many coupling partners toward C−H functionalizations that occurred solely at the *ortho*-positions,[8] raising the question whether the anionic α-O-center was able to

Received: April 30, 2016
Published: July 27, 2016

DOI: 10.1021/acs.joc.6b00997
J. Org. Chem. 2016, 81, 7400−7410

direct the 4-membered cyclopalladation for the pyridine *N*-oxide systems.

The 5-membered and 6-membered cyclopalladations were so prevalent in the C−H activation chemistry[1a] that one may feel neither surprised nor excited about the cross-couplings reacting efficiently at the *ortho*-positions of aromatic rings bearing a *β*- or *γ*-heteroatom. Examples in the literatures covered lots of organic functionalities, such as ketones,[9a−c] esters,[9a,d] carboxylic acids,[9e,f] alcohols,[9g,h] amides,[9i−k] imines,[10a−c] pyridines,[10d−f] oximes,[10g,h] thioethers and phosphines,[11] among which O-containing functionalities were the most frequently used as directing groups, followed by N-containing groups and then the corresponding S- or P-containing groups. The X-ray determinations have already characterized some 5-membered and 6-membered palladacycles as intermediates,[12] which were isolated from the reactions of $Pd(OAc)_2$ with the corresponding aromatic substrates, containing O-, N- or S-center groups, in the absence of coupling partners. Some typical aromatics used in the 5-membered and 6-membered cyclopalladations are given in Scheme 1, in which the observed reaction positions are indicated with red small cycles.

Scheme 1. Some Typical Aromatic Substrates Used in the $Pd(OAc)_2$-Catalyzed C−H Functionalizations with the Observed Reaction Positions Being Indicated

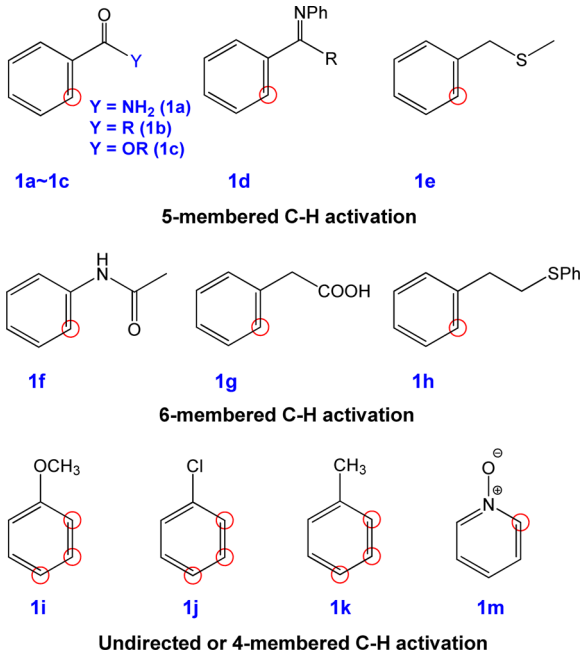

Noteworthy is that the reactant amount used can also be an important determinant of reaction mechanism for a given directing group system. For example, both acetylbenzene derivatives and benzoates displayed boundary chemical behaviors in some $Pd(OAc)_2$-catalyzed C−H functionalizations. The sole *ortho* cross-couplings have commonly been observed under general reaction conditions, whereas mixtures of *o*-, *m*- and *p*-products have been isolated when performing the reactions by the use of excess reactants.[6a,b,7d]

Directing groups with a *δ*-heteroatom were theoretically probable to constitute some 7-membered palladacycles with the $Pd(OAc)_2$ catalyst, and in fact, such 7-membered cyclopalladations have still been far away from being accepted in the Pd-catalyzed C−H activation chemistry.[1a] However, a rather limited number of works have indicated the involvement of 7-membered palladacycles to be possible, where some specialized *δ*-heteroatom based aromatics resulted in the regioselective *ortho* C−H functionalizations. Yu's group, for example, performed the alkenylation reaction of hydrocinnamic acids catalyzed by $Pd(OAc)_2$,[13] indicating that $KHCO_3$ as a base was crucial to afford the desired products in good yields (see Scheme 2), since neither KBr nor KI (actually salt) could

Scheme 2. Two Representative C−C Cross-Coupling Reactions in the Literature Probably Involving the 7-Membered Cyclopalladation Process

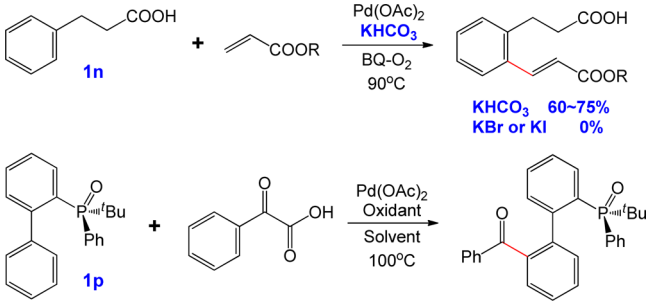

generate any desired products. The same research team also achieved the *ortho* alkenylation, in a similar manner, using the aromatics substituted by a C3 alkyl tether terminated by a sulfonamide group.[14] The observed results could be explained on the basis of 7-membered cyclopalladation pathway induced by a carbonyl oxygen. Yang and co-workers reported, in a recent work, a novel method for the Pd-catalyzed C−H bond acylation of 2-phosphorylbiphenyl to produce some substituted 2′-phosphorylbiphenyl-2-acyl compounds,[15] presenting an unprecedented 7-membered C−H activation process in virtue of the $R_2P{=}O$ directing group (see Scheme 2).

To sum up, C−H bond functionalizations through both 5-membered and 6-membered cyclopalladations have been investigated extensively and developed maturely,[1a] while those via 4-membered or 7-membered cyclopalladations could have only been applied to a rather limited scope of aromatics. Considering the comprehensive exploration of directing group effect by computational method has been rather deficient in the literatures, we therefore use the density functional theory (DFT) calculations to explore, from both kinetic and thermodynamic aspects, the relationships between directing group and chemical reactivity for a series of the $Pd(OAc)_2$-catalyzed C−H activations. Our attention will also be paid to the variation of reaction mechanisms associated with modulation of reaction conditions, such as the ring size of the formed palladacyclic structures, the amount of substrates, and so on. It is our belief that such a comprehensive investigation is crucial and valuable for organic chemists to understand deeply the roles played by different directing group systems.

2. RESULTS AND DISCUSSION

2.1. C−H Activation Mechanisms: Directed and Undirected Pathways. Within the realm of C−H activation chemistry, directing groups refer in particular to the functionalities incorporating with either a *β*- or *γ*-heteroatom (see Scheme 1), due to a clear preference for formation of the 5-membered or 6-membered palladacycles.[1a] While for aromatic substrates bearing an *α*-heteroatom, like anisole and

DOI: 10.1021/acs.joc.6b00997
J. Org. Chem. 2016, 81, 7400−7410

chlorobenzene, the $Pd(OAc)_2$-catalyzed C−H activations are mostly assigned as those without directing group participation,[16] since the supposed 4-membered palladacycles usually have a high degree of stain probably preventing their formation. These mean that there may exist both the directed and undirected pathways for many $Pd(OAc)_2$-catalyzed C−H activation processes, where the competition may be dictated by a combination of several factors, especially the ring size of the palladacyclic structures formed.

In this section, some typical reaction systems visited frequently in the literatures are modeled by using DFT calculations to gain the mechanistic insights into C−H activation pathways. Owing to the diversity of the subsequent transformations happening at the generated C−H activation products, we will select a series of oxidative Heck couplings and other related C−C bond-forming reactions as test benchmarks. Some typical subsequent processes with coupling partners will only be given in the Supporting Information for references.

2.1.1. 5- and 6-Member-Directed C−H Activation Mechanisms. C−H functionalizations directed by a β-heteroatom allow formation of the 5-membered palladacyclic species as intermediate products, which become quite concerned issues in the current C−H activation chemistry.[1a] Among them, benzamide and its derivatives have been the most extensively studied systems in the oxidative Heck couplings, which furnished exclusively the *ortho* alkenylation products in high reaction yields.[9i−k] The following calculations take the reaction of benzamide (**1a**) with $Pd(OAc)_2$ as a model to acquire the kinetic and thermodynamic properties of 5-membered cyclopalladation, as depicted in Figure 1 (in black).

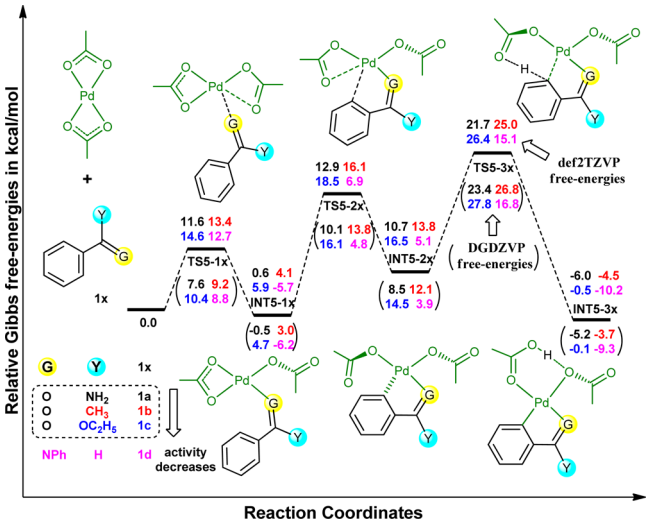

Figure 1. 5-member-directed C−H activation mechanisms for selected aromatics (**1a**, **1b**, **1c** and **1d**) with catalytic $Pd(OAc)_2$. Geometries were optimized at the B3LYP-IDSCRF/DGDZVP level of theory and then single point calculations were carried out using the B3LYP-IDSCRF/def2TZVP theoretical model in DCE solvent. Relative free-energies calculated at the B3LYP-IDSCRF/DGDZVP level of theory were given in the parentheses.

The located reaction mechanisms are generally similar to those reported in many previous theoretical papers,[17] involving multiple elementary steps with the proton-abstraction being rate-limiting. In the first step, **1a** combines with the $Pd(OAc)_2$ catalyst through its carbonyl oxygen exchanging with an O-arm on the κ^2-acetate ligand, forming the initial complex **INT5-1a** via the 5-coordinate transition state **TS5-1a**. Following this, an intramolecular ligand substitution from **INT5-1a** to **INT5-2a** affords the reaction precursor via the transition state **TS5-2a**, from which an O-arm on the other κ^2-acetate ligand is replaced by a benzene *ortho* carbon based on the Pd···π interaction. Subsequently, **INT5-2a** would undergo the proton-abstraction induced by a *cis*-acetate oxygen-atom through a 6-center transition structure **TS5-3a**, itself relaxing to the 5-membered palladacycle **INT5-3a** as the intermediate product.

The free-energy profiles calculated at the B3LYP-IDSCRF/def2TZVP level of theory show that the rate-determining free-energy barrier (**TS5-3a**) is up to 21.7 kcal/mol, readily accessible under mild conditions, and the 5-membered palladacycle **INT5-3a** is obviously more stable with respect to the initial reactants (−6.0 kcal/mol in free-energy). These results can unambiguously support such a 5-membered cyclopalladation to be favorable both kinetically and thermodynamically, and therefore, it is understandable that some structurally related 5-membered palladacyclic intermediates have been isolated and characterized in the stoichiometric syntheses by different research groups.[12]

The relative free-energies obtained from the B3LYP-IDSCRF/DGDZVP method are given in the parentheses, from which one can observe that the basis set effect on relative free-energy is not so obvious, and in most cases, the difference is only ca. 2.0 kcal/mol or less, but it is predicted to be ca. 4.0 kcal/mol more stable for **TS5-1a** using the DGDZVP basis set. In fact, all the reaction systems simulated in this paper display the similar basis set effect, in which the relative free-energies for the rate-determining transition states and the final intermediates are estimated to be rather close between the two basis sets used. Therefore, only the B3LYP-IDSCRF/def2TZVP data will be discussed except noted elsewhere.

Besides **1a**, aromatic ketones (PhCOR) and esters (PhCOOR) were also very important raw materials in many kinds of the Pd-catalyzed C−H functionalizations,[9a−f] most of which presented regioselective *ortho* cross-couplings in support of the 5-member-directed mechanism. Aiming at these systems, we select acetylbenzene (**1b**) and ethyl benzoate (**1c**) as the model reactants to study the C−H activation mechanisms catalyzed by $Pd(OAc)_2$, and the calculation results are provided in Figure 1 with different colors.

Figure 1 clearly shows that modulation of the Y group from NH_2 to CH_3 or to OCH_2CH_3 does not obviously alter the reaction mechanisms but does affect the free-energy profiles, in that the transition states **TS5-3*x*** become higher in free-energy (25.0 and 26.4 kcal/mol for **TS5-3b** and **TS5-3c**) and the cyclopalladation intermediates **INT5-3*x*** coincidentally become less stable (−4.5 and −0.5 kcal/mol for **INT5-3b** and **INT5-3c**). In other words, the overall transformation becomes monotonously more difficult when changing the NH_2 group to CH_3 then to OCH_2CH_3 both kinetically and thermodynamically, resulting in the order of **1a** > **1b** > **1c** for overall reactivity.

The coordination ability of different carbonyl oxygens should be of essential relevance to the observed chemical activity, as the three **INT5-3*x*** (or **TS5-3*x***) structures mainly differ in the nature of the Pd−O coordination bonds formed. Since Pd(II)-O coordination bonds have significant electrostatic and covalent components, the combined natural bond orbital (NBO)[18] and molecular orbital (MO) analyses may provide a deeper understanding on the above results. In general, the larger charge separation between two adjacent atoms is indicative of the stronger inonic attraction formed. It can be

DOI: 10.1021/acs.joc.6b00997
J. Org. Chem. 2016, 81, 7400−7410

noticed from Figure 2 that the NBO charge obtained with B3LYP-IDSCRF/DGDZVP at the carbonyl oxygen of **1b**

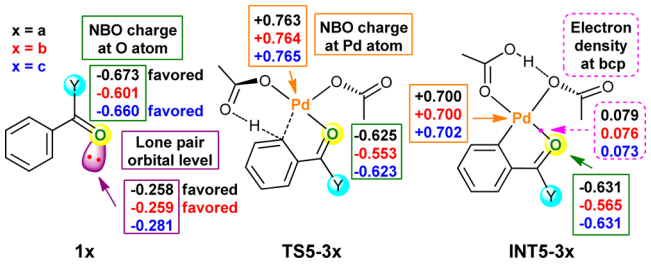

Figure 2. NBO charge distributions at selected atomic centers, energy levels (in au) of lone pair molecular orbitals, and electron density values (in au) at bond critical points for a series of stationary points, calculated at the B3LYP/DGDZVP level of theory. Different colors are used for different reactants (**1a**: black, **1b**: red, **1c**: blue).

(−0.601 e) is evidently less negative than those of **1a** (−0.673 e) and **1c** (−0.660 e), which is in good agreement with the fact that both $-NH_2$ and −OR are good π-electron donor and the former is more pronounced in this aspect. These charges display the similar pattern in the transition states **TS5-3*x*** and intermediates **INT5-3*x***, while the NBO charges at the palladium center seem to be unaffacted by varying substitutents (e.g., +0.763 ∼ +0.765 e for **TS5-3*x*** and +0.700 ∼ +0.702 e for **INT5-3*x***). Therefore, **1b** is predicted to be the least favorable from the NBO charge distributions while both **1a** and **1c** seem to be favorable.

On the other hand, these Pd−O coordination bonds may contain a large percentage of covalent contribution, for which the lone pair orbitals of carbonyl oxygen should mainly be responsible. In this respect, the highest canonical MOs having main character of carbonyl oxygen lone pair are selected for reactants **1a**, **1b** and **1c**, and the corresponding energy levels are list in Figure 2 for comparison. The lone pair orbital of **1c** is observed to be substantially lower-lying with respect to those of **1a** and **1b** (i.e., −0.281 au vs −0.258 and −0.259 au), implying that the carbonyl oxygen of **1c** is less prone to form significant charge transfer interaction with the neighboring palladium center, compared to those of **1a** and **1b**. In summary, both the electrostatic interaction and the orbital interaction are responsible for the reactivity of reactants **1a**, **1b** and **1c**.

In fact, the atoms-in-molecules (AIM) topological analyses may be more straightforward for comparing the relative stability of different Pd−O coordination bonds. The electron density values at the Pd−O bond critical points are calculated to be 0.079, 0.076, and 0.073 au (see Figure 2) for **INT5-3a**, **INT5-3b** and **INT5-3c**, respectively, being parallel with the observed variation in relative free-energies.

Arylketimine (**1d**)[10b,c] has also been modeled as a reactant in our calculations for making a comparison between the O-based and N-based directing groups. The results in Figure 1 (in pink) indicate that all the main stationary points for **1d** system are stabilized by 5−7 kcal/mol in relative free-energy with respect to those for **1a** system, which can be ascribed to the bonding reinforcement of Pd−N relative to Pd−O. Our previous work[5] reported that Pd−N coordination bond is ca. 8−10 kcal/mol inherently stronger than Pd−O for the $Pd(OAc)_2$ catalyst. In addition, benzylmethylsulfide (**1e**), a typical S-center directing group system, shows the similar reactivity to **1d** based on our calculations; detailed information will be given in the Supporting Information.

The corresponding 6-membered cyclopalladations, similar to the 5-membered counterparts, normally require the participation from a γ-heteroatom based directing group to afford the 6-membered palladacyclic species. *N*-phenylacetamide (**1f**) was one of the most prevalent aromatic substrates in the Pd-catalyzed C−H functionalizations,[1c] and the experimental findings exhibited the exclusive *ortho* cross-couplings with good yields.

In general, the 6-membered C−H activation mechanisms are similar to the 5-membered counterparts, since the proton-abstraction transition structure is rate-determining and the formed palladacycle is stable as well. The results show that the reaction of **1f**+$Pd(OAc)_2$ has only the free-energy barrier of 21.2 kcal/mol for proton-abstraction transition state and then lowers the free-energy by 5.0 kcal/mol to yield the 6-membered intermediate product, which should be enough to verify the kinetic and thermodynamic advantages for such a 6-membered pathway. Considering the 6-membered mechanisms have been discussed in a large number of computational works,[17] the detailed reaction pathways and free-energy profiles for **1f**, **1g** and **1h** (see Scheme 1) will only be given in the Supporting Information for saving space.

2.1.2. Undirected C−H Activation Mechanisms. In the literatures, the oxidative Heck reactions, using either anisole or chlorobenzene as one of the reactants, have resulted in mixtures of *o*-, *m*- and *p*-coupling-products,[6] suggesting the undirected C−H activation mechanism was operating, but such syntheses had to be performed by using excess aromatics (usually 10 to 100 equiv). It is particularly true that the nonfunctionalized arenes, such as toluene (**1k**) and other alkylbenzenes,[7] are lack of directing group, and hence only the undirected mechanism can be located (see SI). More interestingly, mixtures of *o*-, *m*- and *p*-coupling-products have been isolated by using excess **1b** and **1c** as substrates, which served as an indicator of the undirected mechanism without carbonyl group participation.[6a,b,7d]

There are a relatively limited number of theoretical works in the literatures[19] dealing with the intermolecular C−H activation without directing group participation, and hence four reactants, such as **1b**, **1c**, anisole (**1i**) and chlorobenzene (**1j**), are selected in this work as the typical aromatic substrates to model the undirected C−H activations (see Figure 3). Since the reaction mechanisms for different reactants **1*x*** (*x* = b, c, i and j) are structurally similar to one another, **1b** is used to describe the optimal reaction channel for the sake of simplicity.

In the first elementary step, one of the four O-arms is removed from the palladium center by the attack of the benzene ring of reactant **1b**, affording the initial complex **INT-1b** via the ligand-exchange transition state **TS-1b**. The orientation of the benzene ring in **INT-1b** is almost perpendicular to the coordination plane, indicative of a kind of Pd···π bonding. Despite the coordination ability of carbonyl oxygen, the absence of any Pd···G interaction between **1b** and $Pd(OAc)_2$ is observed along the reaction coordinates. Therefore, **INT-1b** should serve as the real precursor for the undirected proton-abstraction step.

It is necessary to point out that the intermolecular bonding interaction formed in **INT-1b** is a η^2-style Pd···π coordination involving three distinct modes, i.e., C1−C2, C2−C3, or C3−C4, and hence the *ortho*, *meta*, or *para* C−H bond could be deprotonated, respectively. For simplicity, only the C−H activation mechanism happening at the *ortho* position is shown in Figure 3, which needs to climb up a proton-

DOI: 10.1021/acs.joc.6b00997
J. Org. Chem. 2016, 81, 7400−7410

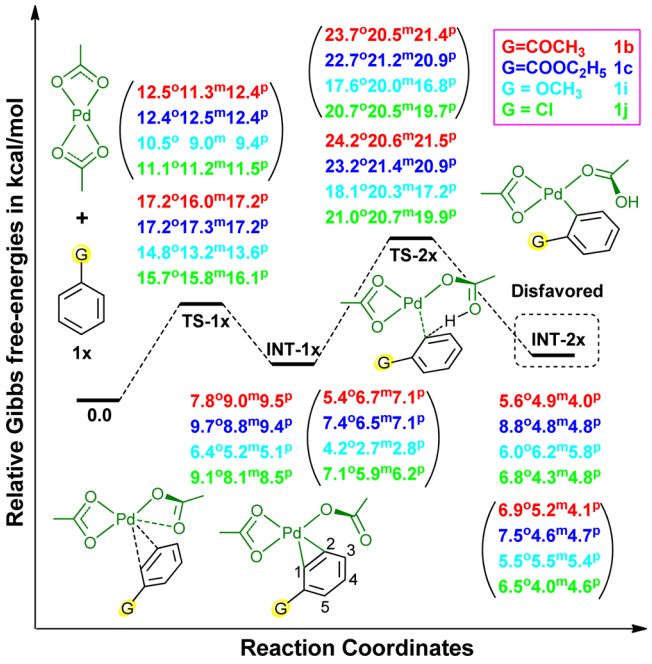

Figure 3. Undirected C−H activation mechanisms for selected aromatics (**1b**, **1c**, **1i** and **1j**) with catalytic $Pd(OAc)_2$. Geometries were optimized at the B3LYP-IDSCRF/DGDZVP level of theory and then single point calculations were carried out using the B3LYP-IDSCRF/def2TZVP theoretical model in DCE solvent. Relative free-energies calculated at the B3LYP-IDSCRF/DGDZVP level of theory were given in the parentheses. Relative free-energies for *ortho*, *meta* and *para* C−H activations were provided with the superscripts *o*, *m* and *p*.

abstraction 6-center transition state **TS-2b**. Subsequently, the open palladation species **INT-2b** is generated as the final intermediate on the undirected pathway.

The free-energy profiles show that the formation of reaction precursors **INT-1*x*** (*x* = b, c, i and j) has to increase the free-energy of 5.1−9.7 kcal/mol, representing a somewhat disfavored process. From a kinetic perspective, the C−H activation steps proceed facilely involving low free-energy barriers (17.2−24.2 kcal/mol) relative to the initial reactants. Nevertheless, the overall free-energy changes are estimated to be 4.0−8.8 kcal/mol, negating the spontaneity for formation of open palladation intermediates under standard conditions. In addition, the main values of the entire free-energy profiles vary only a little with the nature of group G. In the next section, we will discuss the difference between the directed and undirected mechanisms.

2.2. Contrasting the Directed and Undirected Mechanisms. An experimental indicator to make an assignment of reaction mechanism originates from the distributions of coupling-products, because the directed processes normally result in the regioselective *ortho* C−H functionalizations, while the undirected processes should be accompanied by the production of mixtures of *o*-, *m*- and *p*-products. Besides this, one may be eager to contrast the two mechanisms from both kinetic and thermodynamic aspects, in order to reveal the internal relationship between experimental conditions and reaction mechanisms.

As demonstrated earlier, aromatics **1b** and **1c** displayed boundary chemical behaviors associated with modulation of reaction conditions. They reacted with the catalytic $Pd(OAc)_2$ commonly through the 5-member-directed mechanism to afford solely the *ortho* coupling-products;[9a−c] in contrast, the undirected C−H activation pathway was suggested to be more competitive by using excess reactants, and consistently, mixtures of *o*-, *m*-, and *p*-products have been detected.[6a,b,7d]

In order to make clear whether a competition would arise between the directed and undirected pathways for **1b** and **1c**, the corresponding free-energy profiles on the two pathways are comparatively plotted in Figure 4. Obviously, the undirected

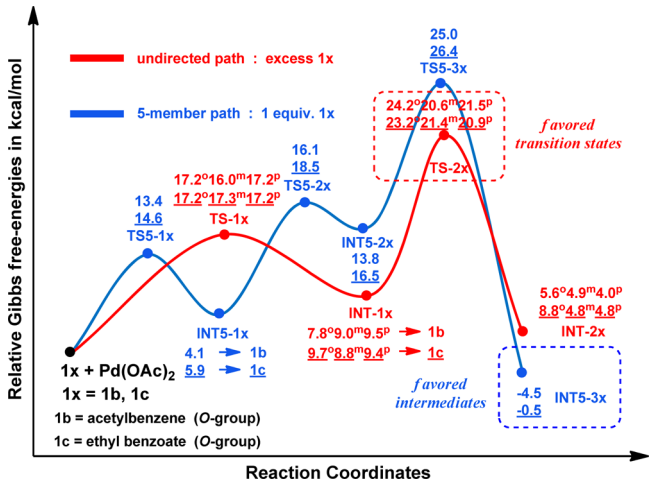

Figure 4. C−H activation mechanisms for **1b** and **1c**: 5-membered pathway directed by weak coordination group (in blue) vs undirected pathway (in red), along with free-energy changes determined at the B3LYP-IDSCRF/def2TZVP level of theory in DCE solvent. Molecular geometries of the involved stationary points were given in Figures 1 and 3.

pathway is a two-step process, whereas the directed pathway is comprised of three elementary steps. More importantly, the transition states **TS5-3*x*** lie higher in free-energy by ca. 1−6 kcal/mol relative to the corresponding **TS-2*x*** structures, indicating the directing group participation seems to increase the free-energy barriers of proton-transfer. The activation free-energy barrier for rate-controlling process should be the free-energy difference between proton transfer transition state and starting materials according to the steady-state approximation.[20] One can perform more detailed kinetic analyses, based on the energetic span model[21] developed by Kozuch and Shaik, to consider the contributions of all the transition states and intermediates to overall rate, from which the similar conclusion could be reached (see SI). Contrastingly, the thermodynamic parameters display the reverse trend, because formation of the 5-membered palladacycles **INT5-3*x*** is estimated to be thermodynamically allowed with negative free-energy changes, whereas that of the open palladation intermediates **INT-2*x*** is evidently endothermal (ΔG = 4−9 kcal/mol) and thus unspontaneous. Generally speaking, mediation of carbonyl directing groups in the C−H activation can stabilize the intermediate products yet may destabilize the proton-transfer transition states.

The competition between the two pathways may be dictated by screening experimental conditions, especially the reactant amount used. Since formation of **INT-2*x*** is via a rapid but endothermic process, the use of an excess amount of reactants could facilitate a forward shift in the chemical equilibrium and would allow the existence of **INT-2*x*** in a low concentration, which actually benefits the following transformations with

DOI: 10.1021/acs.joc.6b00997
J. Org. Chem. 2016, 81, 7400−7410

coupling partners. Our further calculations prove that the migratory insertions of **INT-2*x*** with methyl acrylate, a popular olefinic partner in the Heck couplings, involve moderate activation barriers (9−12 kcal/mol) with lowering the free-energy by more than 10.0 kcal/mol, contributing to overall exothermic catalytic cycles; detailed information on the subsequent processes are available in the Supporting Information. In this regard, therefore, the undirected C−H activation pathway should be recommended on the basis of kinetics.

When using an equivalent amount of reactants, formation of **INT-2*x*** via the undirected pathway seems obviously disfavored from thermodynamics. However, the palladacycles **INT5-3*x*** can be furnished through the 5-member-directed pathway, which climbs up relatively higher free-energy barrier and then leads to overall spontaneous process. Under general reaction conditions, therefore, only the directed pathway is accessible from thermodynamics. The conclusions in this section are in good agreement with the experimental observations.[9a−c,6a,b]

The competition relationship for these two reaction pathways elucidated in Figure 4 is also valid for some other electron-neutral O-center directing group systems, for examples, **1a** and **1f** in Scheme 1; details are available in the Supporting Information.

Noteworthy is that a different competition parttern appears for strong directing group systems, particularly for those containing N- and S-center groups, such as **1d** and **1e** in Scheme 1. The free-energy profiles for the directed and undirected pathways are carefully plotted in Figure 5,

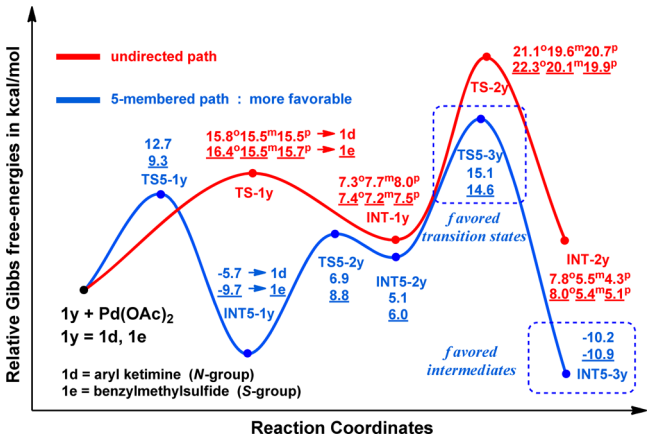

Figure 5. C−H activation mechanisms for **1d** and **1e**: 5-membered pathway directed by strong coordination group (in blue) vs undirected pathway (in red), along with free-energy changes determined at the B3LYP-IDSCRF/def2TZVP level of theory in DCE solvent. Molecular geometries of the involved stationary points were given in Figure 1 and S1.

illustrating the 5-membered pathway becomes more advantageous than the undirected pathway both kinetically and thermodynamically for **1d** and **1e**. This is because the Pd−N and Pd−S coordination bonds are estimated to be ca. 6−10 kcal/mol stronger than the Pd−O,[5] lowering the whole free-energy profiles for the 5-membered pathway.

In brief, a strong directing group can stabilize the proton-transfer transition state whereas a moderate O-center directing group may increase the free-energy barrier of proton-transfer, compared to the undirected C−H activation pathway. After carefully investigating two representative structures of **TS5-3b** and **TS-2b** (see Figure 6), it could be found that the geometrical restriction imposed by the 5-membered cyclic

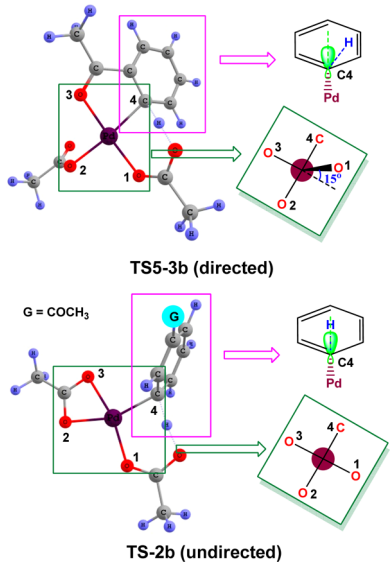

Figure 6. Molecular orientations for the directed transition state (**TS5-3b**) and the undirected transition state (**TS-2b**).

framework would hinder the rotation of the benzene ring along the Pd−C4 bond in **TS5-3b**, and thus substantial steric strain would be present in **TS5-3b** upon the proton-abstraction. For example, the Pd−O1 bond axis deviates from the coordination plane by ca. 15°, and the direction of the C···H incipient bond is unaligned with the sp^3-like orbital at the C4 center, in order to satisfy the C···H···O near linear arrangement. Such nonideal structural parameters diminish gradually as the proton-transfer is completed. In contrast, the undirected transition state **TS-2b** is more flexible, which allows the benzene ring to adopt a perpendicular orientation for maintaining the ideal structural parameters. These feathers are consistent with the observation that **TS5-3b** lies higher in free-energy than **TS-2b**. In fact, such kinds of structural nonideality can also be observed in both **TS5-3d** and **TS5-3e** (see Figure 5), but the stronger coordination bonds of Pd−N and Pd−S dominate over the steric strain present in the directed transition states, leading to that **TS5-3d** and **TS5-3e** become lower in free-energy than **TS-2d** and **TS-2e**, respectively.

2.3. 4-Member-Directed or Undirected Mechanism?

Pyridine *N*-oxide and the derivatives were excellent aromatic substrates for the oxidative Heck couplings,[8] which displayed exceptional chemical reactivity, especially for the C−C cross-couplings happening solely at the *ortho* positions. The experimental findings of product distributions apparently supported the 4-member-directed C−H activation pathway to be plausible, but this mechanism has not been as prevalent as the corresponding 5-membered or 6-membered one. In our opinion, it is necessary to perform DFT calculations on the C−H palladation of pyridine *N*-oxide (**1m**) using the $Pd(OAc)_2$ catalyst to confirm whether the 4-member-directed pathway is actually preferred or not.

The calculation results are presented in Figure 7, from which one can observe that two competing mechanisms, namely, the undirected pathway (in red) and the 4-member-directed pathway (in blue), are both two-step process. In the former mechanism, the initial intermediate **INT-1m** is formed via the

DOI: 10.1021/acs.joc.6b00997
J. Org. Chem. 2016, 81, 7400−7410

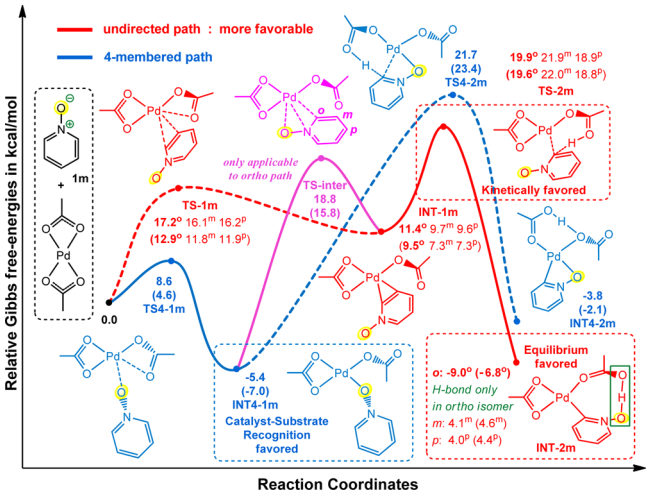

Figure 7. C−H activation mechanisms for **1m** with catalytic $Pd(OAc)_2$: 4-member-directed pathway (in blue) vs undirected pathway (in red). Geometries were optimized at the B3LYP-IDSCRF/DGDZVP level of theory and then single point calculations were carried out using the B3LYP-IDSCRF/def2TZVP theoretical model in DCE solvent. Relative free-energies calculated at the B3LYP-IDSCRF/DGDZVP level of theory were given in the parentheses. Relative free-energies for undirected *ortho*, *meta* and *para* C−H activations were provided with the superscripts *o*, *m* and *p*.

transition state **TS-1m**, indicative of a typical Pd···π interaction with the pyridine ring. Then the proton-transfer step occurs via the open transition state **TS-2m**, which affords the open palladation species **INT-2m** with a strong O−H···O hydrogen-bond present only in the *ortho* product. In the latter mechanism, the coordination of **1m** with the catalyst $Pd(OAc)_2$ is based on the anionic oxygen, leading to the intermediate **INT4-1m** as the precursor. Subsequently, the 4-member-directed C−H activation step passes through the transition state **TS4-2m** to obtain the 4-membered palladacycle **INT4-2m**.

The difference in the first step is that formation of **INT4-1m** is favorable (ΔG = −5.4 kcal/mol), whereas that of **INT-1m** is obviously endothermal (ΔG = +11.4 kcal/mol), meaning that the former intermediate is more probable as the precursor arising from the stronger coordination of the anionic oxygen. Therefore, the catalyst-substrate recognition should originate from the interaction of Pd···O^-, generating the encounter intermediate **INT4-1m** via the transition state **TS4-1m**.

The C−H activation step on the directed pathway, however, seems relatively unfavorable, since the free-energy barrier for rate-controlling step (**TS4-2m**) is 21.7 kcal/mol relative to the starting point, 1.8 kcal/mol higher than that of **TS-2m**. In addition, the **INT4-2m** species generated is also less stable than the *ortho* palladation intermediate **INT-2m** (−3.8 vs −9.0 kcal/mol in free-energy).

It is interesting that a transition state **INT-inter**, for the interconversion between **INT4-1m** and **INT-1m**, could be located, with the relative free-energy being 18.8 kcal/mol. This transition state lies below both **TS-2m** and **TS4-2m**, implying that this ligand isomerization **INT4-1m** → **INT-1m** should be prior to the proton-abstraction from kinetics. So actually, the two reaction channels are interlinked by such an interconversion process shown as the pink curve in Figure 7. In this manner, the most probable reaction route can be obtained as follows: $Pd(OAc)_2$+**1m** → **TS4-1m** → **INT4-1m** → **TS-inter** → **INT-1m** → **TS-2m** → **INT-2m**, as presented with the solid curve.

It remains a question why the C−C cross-couplings could happen solely at the *ortho* positions of **1m** judging from such a mixed reaction mechanism. One can realize from Figure 7 that only the *ortho* isomer of **INT-2m** is relatively stable with respect to the initial reactants, because a very strong N—O···H···O=C hydrogen-bond is formed between the acetic acid ligand and the anionic oxygen. The distances of N—O···H and H···O=C are calculated to be 1.06 and 1.47 Å, respectively, indicating that the hydrogen atom lies closer to the anionic oxygen center. However, such kind of hydrogen-bond is absent in both the *meta* and *para* isomers of **INT-2m**, due to the longer distance between the two oxygen centers. It can be stated that the *ortho* directing effect in **1m** lies after the proton-abstraction transition state, in which formation of the strong hydrogen-bond should be responsible for the observed regioselectivity.

One can observe from Figure 7 that the 4-membered palladacyclic species (**INT4-2m**) is relatively stable after passing over a higher activation barrier, since the strong coordination of anionic oxygen can compensate the high degree of strain developed in the 4-membered ring to make up an overall stabilization. If the α-oxygen becomes an electron-neutral heteroatom, like that in **1i**, such a 4-membered mechanism can be surely precluded. For example, our calculations have also tested this mechanism using the model reaction of **1i**+$Pd(OAc)_2$, which needs to overcome a free-energy barrier of 36.4 kcal/mol to form the 4-membered intermediate with an endothermal free-energy of 11.5 kcal/mol. Therefore, the undirected mechanism seems to be the only candidate for the **1i**+$Pd(OAc)_2$ reaction system; detailed information will be given in the Supporting Information.

2.4. 7-Member-Directed Mechanism. Actually, the 7-membered cyclopalladation via C−H activation was quite uncommon and challenging in the Pd-catalyzed syntheses. In the literatures, however, a rather limited number of synthetic works have indicated the possibility of the involvement of 7-membered cyclopalladation.[13−15]

The first reaction in Scheme 2 is an oxidative Heck coupling of 3-phenyl propionate acids (**1n**) promoted by $KHCO_3$ as a base, and under such conditions, **1n** could be deprotonated to form the corresponding potassium propionate species (**1o**). Since this acid−base neutralization is irreversible and very fast, **1n** should turn into **1o** completely prior to reacting with the catalyst, and thus the functional group becomes COO^-K^+ from COOH, as shown in Figure 8(a).

The free-energy variation in Figure 9 validates the accessibility of this transformation (red curve), showing the overall process is clearly spontaneous (ΔG = −7.3 kcal/mol) without any high-lying transition state. These theoretical results are in good agreement with the experimentally determined chemical reactivity.[13]

In order to explain the role of base, the corresponding process of **1n** with $Pd(OAc)_2$ has comparatively been plotted in Figure 9 (green curve), from which one can see that all the main stationary points are dramatically destabilized in the absence of $KHCO_3$. After **TS7-1n**, all the stationary points for the $Pd(OAc)_2$+**1n** system lie 13−16 kcal/mol above the counterparts for the $Pd(OAc)_2$+**1o** system, and especially, the relative free-energy of **INT7-3n** is 7.0 kcal/mol above the initial reactants, leading to that only the base-involved system can

DOI: 10.1021/acs.joc.6b00997
J. Org. Chem. 2016, 81, 7400−7410

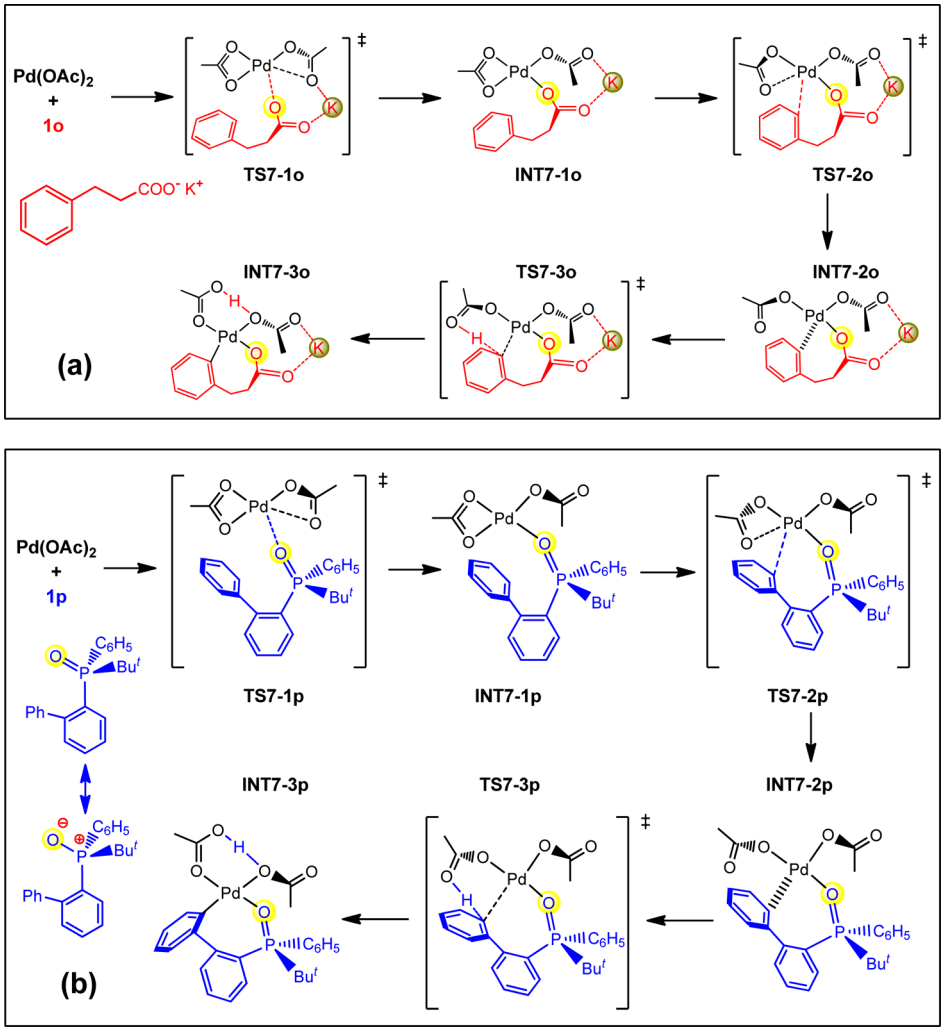

Figure 8. 7-Member-directed C−H activation mechanisms for **1o** (top) and **1p** (bottom) with catalytic $Pd(OAc)_2$, optimized at the B3LYP-IDSCRF/DGDZVP level of theory in DCE solvent.

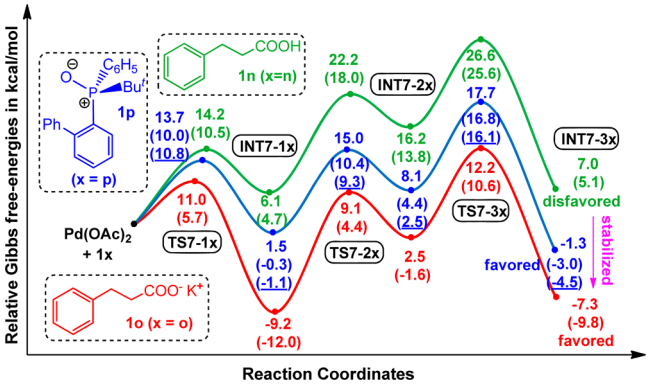

Figure 9. Gibbs free-energy profiles for the 7-membered C−H activations with **1n** (green), **1o** (red) and **1p** (blue) as substrates, determined at the B3LYP-IDSCRF/def2TZVP level of theory in DCE solvent. Values in the parentheses were derived from the B3LYP-IDSCRF/DGDZVP calculations, and those underlined were obtained in acetonitrile solvent. Molecular geometries of the involved stationary points were given in Figure 8.

promote the 7-membered cyclopalladation from thermodynamics.

The above discussion confirms that the anionic carboxylate group is more suitable for directing the uncommon 7-membered process with comparison to the neutral carboxyl group, in which the stability of intermediate palladacyclic species is a key problem. In order to rationalize this effect, the molecular geometries and electron topological graphs for the formed intermediate products **INT7-3*x*** (*x* = n, o, p) are depicted in Figure 10, from which one can notice that such 7-membered palladacycles are obviously puckered, i.e., substantial distortion strain would be imposed on these structures. Therefore, it is not difficult to understand that they are destabilized in free-energy change for electron-neutral directing groups (e.g., neutral O-center group in **1n**). However, if it is for electron-rich directing groups (e.g., anionic O-center group in **1o**), the stronger coordination bond could overwhelm the distortion strain and stabilize the intermediate products. This is evidenced by the change of Pd−O1 bond length from 2.16 Å in **INT7-3n** to 2.10 Å in **INT7-3o**, which is parallel with the change of electron density at the bond critical point (0.0647 and 0.0794 au for **INT7-3n** and **INT7-3o**, respectively). This stabilizing effect is further reinforced by the electrostatic interaction originating from some loose K···O contacts present in both the transition states and intermediates.

DOI: 10.1021/acs.joc.6b00997
J. Org. Chem. 2016, 81, 7400−7410

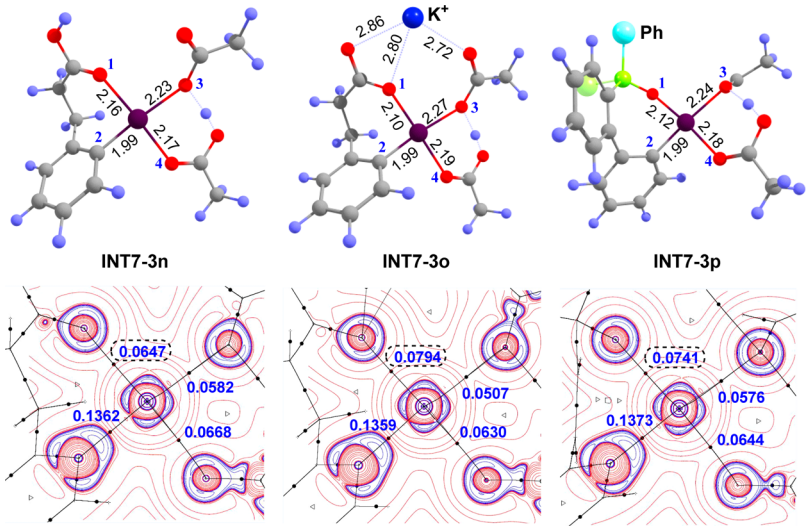

Figure 10. 3D structures and ORTEP plots of three selected 7-membered palladacycles: **INT7-3n** (left), **INT7-3o** (middle) and **INT7-3p** (right), calculated at the B3LYP/DGDZVP level of theory. Depiction of the "onion layer" 2-D isodensity surfaces were provided from the Laplacian of electron densities ($\nabla^2\rho$) in the selected plane, with the bond lengths (Å), bond paths, electron densities (ρ_b in au) and bond critical points are shown in black text, solid black line, blue text and small black dot, respectively.

The last focus is a currently published $Pd(OAc)_2$-catalyzed C−H acylation of 2-phosphorylbiphenyl (**1p**),[15] involving a novel $R_2P{=}O$-directed 7-membered C−H activation process (see Scheme 2). It has been, of course, selected as a typical example in the exploration of 7-membered cyclopalladation with the proposed reaction mechanism being provided in Figure 8(b). The resonance structures ($P{=}O \leftrightarrow P^+{-}O^-$) of **1p** indicate that the central oxygen has a partially anionic nature, which may be pivotal for stabilizing the final intermediate as shown in Figure 9 (blue curve). Similarly, the proton-abstraction transition state **TS7-3p** is rate-determining, only with a free-energy barrier of 17.7 kcal/mol, according to the steady-state approximation.[20] Importantly, the 7-membered cyclopalladation product **INT7-3p** is relatively stable by 1.3 kcal/mol in free-energy, demonstrating the spontaneity and accessibility for this process.

In fact, acetonitrile was proved as the most efficient solvent for the $Pd(OAc)_2$-catalyzed C−H acylation of **1p** in a recent paper,[15] and therefore, the relative free-energies calculated in acetonitrile were given in Figure 9 (the values underlined) with comparison to those obtained in DCE, a common solvent used in the present study. Computationally, the solvent effect on energetic data is not evident for the studied C−H activations using the PCM implicit solvation method (see the Computational Details), for example, the free-energies of **TS7-3p** and **INT7-3p** are 0.7 and 1.5 kcal/mol lower in acetonitrile than in DCE, respectively. Further calculations based on the PCM method demonstrated that only trivial deviation in free-energy would be caused by using some other popular solvents, such as toluene, THF and DMF (see SI). In order to make sure that the estimated free-energy differences do not contain any solvation contribution, DCE is selected as the common solvent in all the calculations.

In summary, an electron-rich directing group can overwhelm the energy cost associated with generation of unusual ring through forming a stronger coordination bond, facilitating a thermodynamically favorable transformation. We have also designed some other β-phenyl carbonyl derivatives, like 4-phenyl-2-butanone (**1l**, see SI), in 7-membered processes, and the obtained results turned out that formation of 7-membered palladacycles is essentially disfavored from thermodynamics as visited in the **1n**+$Pd(OAc)_2$ process, proving the inherent destabilization of 7-membered palladacyclic species incorporating with an electron-neutral oxygen.

3. CONCLUSIONS

A series of the $Pd(OAc)_2$-catalyzed C−H activations have been explored by using DFT calculations, with main attention to the directing group and the formed ring size effects occurring in these systems. The following conclusions have been reached:

(1) Mediation of weak directing groups (e.g., neutral O-center groups) can stabilize the cyclopalladation intermediates but would destabilize the proton-transfer transition states, whereas both the proton-transfer transition states and the cyclopalladation intermediates can be stabilized with the assistance of stronger directing groups (such as N- and S-center groups).

(2) A shift of reaction pathway from the 5-member-directed to the undirected is predicted in our calculations when an excess amount of **1b** or **1c** are used, being parallel with the experimental observations.

(3) The regioselective *ortho* C−H functionalizations on pyridine *N*-oxides should be explained based on the undirected C−H activation pathway, since it was calculated to be more accessible both thermodynamically and kinetically compared to the 4-member-directed pathway.

(4) Employing electron-rich directing groups can help to stabilize the cyclopalladation intermediates formed and thus to facilitate the unusual 7-membered C−H activation processes.

4. COMPUTATIONAL DETAILS

All minima and saddle-point geometries were optimized with the B3LYP method as implemented in Gaussian 09,[22] employing the standard double-ζ valence polarized all-electron DGDZVP basis set for all the metal and nonmetal atoms.[23] The default self-consistent reaction field (SCRF) polarizable continuum model (PCM)[24] was

DOI: 10.1021/acs.joc.6b00997
J. Org. Chem. 2016, 81, 7400−7410

used with dichloroethane (DCE) as a common solvent, while our IDSCRF radii[25] were chosen as the atomic radii to define the molecular cavity, denoted as B3LYP-IDSCRF in this paper. All the optimized stationary points were subsequently characterized by frequency analyses, from which the zero-point energies were obtained for calculating the total energies, in addition to ensuring that all the resultant structures resided at minima or first-order saddle points on the potential energy surfaces. Intrinsic reaction coordinate (IRC)[26a] computations with the Hessian-based predictor−corrector integrator (HPC)[26b,c] were also used to trace some suspected reaction paths to confirm the optimized transition states as being on the correct reaction coordinates. In addition, solution translational entropy calculations have been carried out using our THERMO program,[27] in order to get more accurate relative free-energies for solution reaction systems.

Single point calculations have been performed using the def2TZVP basis set for all elements,[28] based on the B3LYP-IDSCRF/DGDZVP optimized geometries, to further refine the free-energies obtained. Some selected model reaction systems have been reoptimized and characterized using some dispersion-corrected density functionals, such as the B3LYP+D3[29] and M06,[30] in order to validate the density functional used. For most stationary points in this article, both the B3LYP+D3 and M06 predicted much lower relative free-energies (5−15 kcal/mol) with comparison to the B3LYP. Using some experimentally determined free-energy barriers of C−H activation process as test benchmarks, the B3LYP method generated the most satisfactory kinetic parameters (see Figure S7). Besides, the B3LYP method predicted the instability of open palladation species, consistent with the literature reports[12] that only cyclopalladation intermediates had been isolated so far under stoichiometric C−H activation conditions, whereas the other two methods suggested the modest stability of open palladation structures (see Table S4).

The electronic structures of selected stationary points were analyzed by Bader's atoms-in-molecules (AIM)[31] theory, to quantitatively characterize the topological properties of the electron density distributions. Analyses were performed on the wave functions derived from the B3LYP-IDSCRF/DGDZVP method on the optimized geometries. All molecular graphs and 2-dimensional Laplacian reported in this work have been performed with the AIM98PC[32] program package, a modified version of the AIMPAC program.[33]

■ ASSOCIATED CONTENT

Supporting Information

The Supporting Information is available free of charge on the ACS Publications website at DOI: 10.1021/acs.joc.6b00997.

The optimized geometric parameters for all stationary points; the vibrational frequencies; the electronic energies, zero-point energies and total free energies; the complementary mechanistic characterizations and computational methods (PDF)

■ AUTHOR INFORMATION

Corresponding Author

*E-mail: dcfang@bnu.edu.cn.

Notes

The authors declare no competing financial interest.

■ ACKNOWLEDGMENTS

This work was supported by the National Natural Science Fundation of China (21373030).

■ REFERENCES

(1) (a) Chen, X.; Engle, K. M.; Wang, D.-H.; Yu, J.-Q. *Angew. Chem., Int. Ed.* **2009**, *48*, 5094−5115. (b) Aguilar, D.; Cuesta, L.; Nieto, S.; Serrano, E.; Urriolabeitia, E. P. *Curr. Org. Chem.* **2011**, *15*, 3441−3464. (c) Le Bras, J.; Muzart, J. *Chem. Rev.* **2011**, *111*, 1170−1214. (d) Lyons, T. W.; Sanford, M. S. *Chem. Rev.* **2010**, *110*, 1147−1169. (e) Gensch, T.; Hopkinson, M. N.; Glorius, F.; Wencel-Delord, J. *Chem. Soc. Rev.* **2016**, *45*, 2900−2936. (f) Zhang, F.-L.; Hong, K.; Li, T.-J.; Park, H.; Yu, J.-Q. *Science* **2016**, *351*, 252−256. (g) He, G.; Wang, B.; Nack, W. A.; Chen, G. *Acc. Chem. Res.* **2016**, *49*, 635−645.

(2) (a) Cho, S. H.; Ji, Y. K.; Kwak, J.; Chang, S. *Chem. Soc. Rev.* **2011**, *40*, 5068−83. (b) Joanna, W. D.; Thomas, D.; Fan, L.; Frank, G. *Chem. Soc. Rev.* **2011**, *40*, 4740−4761. (c) Zhang, F.; Spring, D. R. *Chem. Soc. Rev.* **2014**, *43*, 6906−6919.

(3) (a) Roglans, A.; Pla-Quintana, A.; Moreno-Manas, M. *Chem. Rev.* **2006**, *106*, 4622−4643. (b) Denmark, S. E.; Regens, C. S. *Acc. Chem. Res.* **2009**, *40*, 1486−1499. (c) Ros, A.; Fernández, R.; Lassaletta. *Chem. Soc. Rev.* **2014**, *43*, 3229−3243. (d) Zhang, M.; Zhang, Y.; Jie, X.; Zhao, H.; Li, G.; Su, W. *Org. Chem. Front.* **2014**, *1*, 843−895. (e) Sun, C. L.; Li, B. J.; Shi, Z. J. *Chem. Commun.* **2010**, *46*, 677−685. (f) Engle, K. M.; Mei, T. S.; Wasa, M.; Yu, J. Q. *Acc. Chem. Res.* **2011**, *45*, 788−802. (g) Jazzar, R.; Hitce, J.; Renaudat, A.; Sofack-Kreutzer, J.; Baudoin, O. *Chem. - Eur. J.* **2010**, *16*, 2654−2672.

(4) (a) Whisler, M. C.; MacNeil, S.; Snieckus, V.; Beak, P. *Angew. Chem., Int. Ed.* **2004**, *43*, 2206−2225. (b) Chen, Z.; Wang, B.; Zhang, J.; Yu, W.; Liu, Z.; Zhang, Y. *Org. Chem. Front.* **2015**, *2*, 1107−1295.

(5) Zhang, L.; Fang, D. C. *Org. Biomol. Chem.* **2015**, *13*, 7950−7960.

(6) (a) Pan, D.; Yu, M.; Chen, W.; Jiao, N. *Chem. - Asian J.* **2010**, *5*, 1090−1093. (b) Pan, D.; Jiao, N. *Synlett* **2010**, *2010*, 1577−1588. (c) Rodriguez, A.; Moran, W. J. *Eur. J. Org. Chem.* **2009**, *2009*, 1313−1316. (d) Obora, Y.; Okabe, Y.; Ishii, Y. *Org. Biomol. Chem.* **2010**, *8*, 4071−4073. (e) Zhou, L.; Lu, W. *Organometallics* **2012**, *31*, 2124−2127. (f) Chung, L. G. Y.; Juwaini, N. A. B.; Seayad, J. *ChemCatChem* **2015**, *7*, 1270−1274. (g) Ricci, P.; Krämer, K.; Larrosa, I. *J. Am. Chem. Soc.* **2014**, *136*, 18082−18086.

(7) (a) Tani, M.; Sakaguchi, S.; Ishii, Y. *J. Org. Chem.* **2004**, *69*, 1221−1226. (b) Yokota, T.; Tani, M.; Sakaguchi, S.; Ishii, Y. *J. Am. Chem. Soc.* **2003**, *125*, 1476−1477. (c) Yamada, T.; Sakaguchi, S.; Ishii, Y. *J. Org. Chem.* **2005**, *70*, 5471−5474. (d) Zhang, Y.-H.; Shi, B.-F.; Yu, J.-Q. *J. Am. Chem. Soc.* **2009**, *131*, 5072−5074. (e) Juwaini, N. A. B.; Ng, J. K. P.; Seayad, J. *ACS Catal.* **2012**, *2*, 1787−1791. (f) Wu, J.; Hoang, K. L. M.; Leow, M. L.; Liu, X.-W. *Org. Chem. Front.* **2015**, *2*, 502−505.

(8) (a) Cho, S. H.; Hwang, S. J.; Chang, S. *J. Am. Chem. Soc.* **2008**, *130*, 9254−9256. (b) Campeau, L.-C.; Schipper, D. J.; Fagnou, K. *J. Am. Chem. Soc.* **2008**, *130*, 3266−3267. (c) Gong, X.; Song, G.; Zhang, H.; Li, X. *Org. Lett.* **2011**, *13*, 1766−1769. (d) Xiao, B.; Liu, Z.-J.; Liu, L.; Fu, Y. *J. Am. Chem. Soc.* **2013**, *135*, 616−619. (e) Wu, J.; Cui, X.; Chen, L.; Jiang, G.; Wu, Y. *J. Am. Chem. Soc.* **2009**, *131*, 13888−13889. (f) Sun, W.; Wang, M.; Zhang, Y.; Wang, L. *Org. Lett.* **2015**, *17*, 426−429.

(9) (a) Shan, G.; Yang, X.; Ma, L.; Rao, Y. *Angew. Chem.* **2012**, *124*, 13247−13251. (b) Choy, P. Y.; Kwong, F. Y. *Org. Lett.* **2013**, *15*, 270−273. (c) Li, G.; Wan, Li.; Zhang, G.; Leow, D.; Spangler, J.; Yu, J.-Q. J. *J. Am. Chem. Soc.* **2015**, *137*, 4391−4397. (d) Sun, X.; Shan, G.; Sun, Y.; Rao, Y. *Angew. Chem., Int. Ed.* **2013**, *52*, 4440−4444. (e) Zhu, C.; Zhang, Y.; Kan, J.; Zhao, H.; Su, W. *Org. Lett.* **2015**, *17*, 3418−3421. (f) Shi, B.-F.; Zhang, Y.-H.; Lam, J. K.; Wang, D.-H.; Yu, J.-Q. *J. Am. Chem. Soc.* **2010**, *132*, 460−461. (g) Wang, X.; Lu, Y.; Dai, H. X.; Yu, J. Q. *J. Am. Chem. Soc.* **2010**, *132*, 12203−12205. (h) Lu, Y.; Leow, D.; Wang, X.; Engle, K. M.; Yu, J.-Q. *Chem. Sci.* **2011**, *2*, 967−971. (i) Li, D.-D.; Yuan, T.-T.; Wang, G.-W. *J. Org. Chem.* **2012**, *77*, 3341−3347. (j) Wang, G.-W.; Yuan, T.-T. *J. Org. Chem.* **2010**, *75*, 476. (k) Dai, H.-X.; Yu, J.-Q. *J. Am. Chem. Soc.* **2012**, *134*, 134−137.

(10) (a) Lim, S. G.; Ahn, J. A.; Jun, C. H. *Org. Lett.* **2009**, *11*, 1317−1320. (b) Tredwell, M. J.; Gulias, M.; Bremeyer, N. G.; Johansson, C. C. C.; Collins, B. S. L.; Gaunt, M. J. *Angew. Chem., Int. Ed.* **2011**, *50*, 1076−1079. (c) Shao, J.; Chen, W.; Giulianotti, M. A.; Houghten, R. A.; Yu, Y. *Org. Lett.* **2012**, *14*, 5452−5455. (d) Wang, Z.; Kuninobu, Y.; Kanai, M. *J. Am. Chem. Soc.* **2015**, *137*, 6140−6143. (e) Xu, C.; Shen, Q. *Org. Lett.* **2014**, *16*, 2046−2049. (f) Hull, K. L.; Sanford, M. S. *J. Am. Chem. Soc.* **2007**, *129*, 11904−11905. (g) Li, Z.-Y.; Wang, G.-W. *Org. Lett.* **2015**, *17*, 4866−4869. (h) Chan, C.-W.; Zhou, Z.; Chan, A. S. C.; Yu, W.-Y. *Org. Lett.* **2010**, *12*, 3926−3929.

DOI: 10.1021/acs.joc.6b00997
J. Org. Chem. 2016, 81, 7400−7410

(11) (a) Xu, B.; Liu, W.; Kuang, C. *Eur. J. Org. Chem.* **2014**, *2014*, 2576−2583. (b) Wang, B.; Lin, C.; Liu, Y.; Fan, Z.; Liu, Z.; Zhang, Y. *Org. Chem. Front.* **2015**, *2*, 973−977. (c) Beller, M.; Fischer, H.; Herrmann, W. A.; Öfele, K.; Brossmer, C. *Angew. Chem., Int. Ed. Engl.* **1995**, *34*, 1848−1849.
(12) (a) Giri, R.; Yu, J.-Q. *J. Am. Chem. Soc.* **2008**, *130*, 14082−14083. (b) Giri, R.; Liang, J.; Lei, J.-G.; Li, J.-J.; Wang, D.-H.; Chen, X.; Naggar, I. C.; Guo, C.; Foxman, B. M.; Yu, J.-Q. *Angew. Chem., Int. Ed.* **2005**, *44*, 7420−7424. (c) Yu, M.; Xie, Y.; Xie, C.; Zhang, Y. *Org. Lett.* **2012**, *14*, 2164−2167. (d) Racowski, J. M.; Ball, N. D.; Sanford, M. S. *J. Am. Chem. Soc.* **2011**, *133*, 18022−18025. (e) Giri, R.; Chen, X.; Yu, J.-Q. *Angew. Chem.* **2005**, *117*, 2150−2153. (f) Granell, J.; Martínez, M. *Dalton Trans.* **2012**, *41*, 11243−11258. (g) Laga, E.; García-Montero, A.; et al. *Chem. - Eur. J.* **2013**, *19*, 17398−17412.
(13) (a) Wang, D.-H.; Engle, K. M.; Shi, B.-F.; Yu, J.-Q. *Science* **2010**, *327*, 315−319. (b) Engle, K. M.; Wang, D.-H.; Yu, J.-Q. *Angew. Chem., Int. Ed.* **2010**, *49*, 6169−6173.
(14) Li, J.-J.; Mei, T.-S.; Yu, J.-Q. *Angew. Chem., Int. Ed.* **2008**, *47*, 6452−6455.
(15) (a) Ma, Y.-N.; Tian, Q.-P.; Zhang, H.-Y.; Zhou, A.-X.; Yang, S.-D. *Org. Chem. Front.* **2014**, *1*, 284−288. (b) Ma, Y.-N.; Zhang, H.-Y.; Yang, S.-D. *Org. Lett.* **2015**, *17*, 2034−2037.
(16) Kuhl, N.; Hopkinson, M. N.; Wencel-Delord, J.; Glorius, F. *Angew. Chem., Int. Ed.* **2012**, *51*, 10236−10254.
(17) (a) Zhang, L.; Fang, D.-C. *J. Org. Chem.* **2013**, *78*, 2405−2412. (b) Balcells, D.; Clot, E.; Eisenstein, O. *Chem. Rev.* **2010**, *110*, 749−823. (c) Davies, D. L.; Donald, S. M.; Macgregor, S. A. *J. Am. Chem. Soc.* **2005**, *127*, 13754−13755. (d) Biswas, B.; Sugimoto, M.; Sakaki, S. *Organometallics* **2000**, *19*, 3895−3908. (e) Aguilar, D.; Bielsa, R.; Contel, M.; Lledós, A.; Navarro, R.; Soler, T.; Urriolabeitia, E. P. *Organometallics* **2008**, *27*, 2929−2936. (f) Lian, B.; Zhang, L.; Chass, G. A.; Fang, D. C. *J. Org. Chem.* **2013**, *78*, 8376−8385. (g) Sperger, T.; Sanhueza, I. A.; Kalvet, I.; Schoenebeck, F. *Chem. Rev.* **2015**, *115*, 9532−9586.
(18) (a) Foster, J. P.; Weinhold, F. *J. Am. Chem. Soc.* **1980**, *102*, 7211−7218. (b) Reed, A. E.; Weinhold, F. *J. Chem. Phys.* **1983**, *78*, 4066−4073.
(19) Gorelsky, S. I. *Coord. Chem. Rev.* **2013**, *257*, 153−164.
(20) (a) Volk, L.; Richardson, W.; Lau, K. H.; Hall, M.; Lin, S. L. *J. Chem. Educ.* **1977**, *54*, 95−97. (b) Meek, S. J.; Pitman, C. L.; Miller, A. J. M. *J. Chem. Educ.* **2016**, *93*, 275−286.
(21) (a) Kozuch, S.; Shaik, S. *J. Am. Chem. Soc.* **2006**, *128*, 3355−3365. (b) Kozuch, S.; Shaik, S. *J. Phys. Chem. A* **2008**, *112*, 6032−6041.
(22) Frisch, M. J.; Trucks, G. W.; Schlegel, H. B.; Scuseria, G. E.; Robb, M. A.; Cheeseman, J. R.; Scalmani, G.; Barone, V.; Mennucci, B.; Petersson, G. A.; Nakatsuji, H.; Caricato, M.; Li, X.; Hratchian, H. P.; Izmaylov, A. F.; Bloino, J.; Zheng, G.; Sonnenberg, J. L.; Hada, M.; Ehara, M.; Toyota, K.; Fukuda, R.; Hasegawa, J.; Ishida, M.; Nakajima, T.; Honda, Y.; Kitao, O.; Nakai, H.; Vreven, T.; Montgomery, J. A., Jr.; Peralta, J. E.; Ogliaro, F.; Bearpark, M.; Heyd, J. J.; Brothers, E.; Kudin, K. N.; Staroverov, V. N.; Kobayashi, R.; Normand, J.; Raghavachari, K.; Rendell, A.; Burant, J. C.; Iyengar, S. S.; Tomasi, J.; Cossi, M.; Rega, N.; Millam, J. M.; Klene, M.; Knox, J. E.; Cross, J. B.; Bakken, V.; Adamo, C.; Jaramillo, J.; Gomperts, R.; Stratmann, R. E.; Yazyev, O.; Austin, A. J.; Cammi, R.; Pomelli, C.; Ochterski, J. W.; Martin, R. L.; Morokuma, K.; Zakrzewski, V. G.; Voth, G. A.; Salvador, P.; Dannenberg, J. J.; Dapprich, S.; Daniels, A. D.; Farkas, O.; Foresman, J. B.; Ortiz, J. V.; Cioslowski, J.; Fox, D. J. *Gaussian 09*, Revision A.02, Gaussian, Inc.: Wallingford, CT, 2009.
(23) (a) Godbout, N.; Salahub, D. R.; Andzelm, J.; Wimmer, E. *Can. J. Chem.* **1992**, *70*, 560−571. (b) Sosa, C.; Lee, C. *J. Phys. Chem.* **1992**, *96*, 6630−6636.
(24) Scalmani, G.; Frisch, M. J. *J. Chem. Phys.* **2010**, *132*, 114110−114124.
(25) (a) Tao, J. Y.; Mu, W. H.; Chass, G. A.; Tang, T.-H.; Fang, D.-C. *Int. J. Quantum Chem.* **2013**, *113*, 975−984. (b) Fang, D.-C. *SCRF-RADII*; Beijing Normal University: Beijing, China; free of charge for academic users.
(26) (a) Fukui, K. *Acc. Chem. Res.* **1981**, *14*, 363−368. (b) Hratchian, H. P.; Schlegel, H. B. *J. Chem. Phys.* **2004**, *120*, 9918−9924. (c) Hratchian, H. P.; Schlegel, H. B. *J. Chem. Theory Comput.* **2005**, *1*, 61−69.
(27) Fang, D. C. *THERMO Program*, Beijing Normal University: Beijing, China; free of charge for academic users.
(28) (a) Weigend, F.; Ahlrichs, R. *Phys. Chem. Chem. Phys.* **2005**, *7*, 3297−3305. (b) Weigend, F. *Phys. Chem. Chem. Phys.* **2006**, *8*, 1057−1065.
(29) (a) Grimme, S. *J. Comput. Chem.* **2006**, *27*, 1787−1799. (b) Grimme, S.; Antony, J.; Ehrlich, S.; Krieg, H. *J. Chem. Phys.* **2010**, *132*, 154104.
(30) Zhao, Y.; Truhlar, D. G. *J. Chem. Phys.* **2006**, *125*, 194101−194118.
(31) Bader, R. F. W. In *Atoms in Molecules: A Quantum Theory*; Oxford University Press: Oxford, U.K., 1990.
(32) Fang, D. C.; Tang, T. H. *AIM98PC*; Beijing Normal University: Beijing, China, 1998.
(33) *AIMPAC*; McMaster University: Hamilton, Ontario, Canada; available from Professor Bader's Laboratory.

DOI: 10.1021/acs.joc.6b00997
J. Org. Chem. 2016, 81, 7400−7410